UC Santa Barbara
UC Santa Barbara Previously Published Works

Title
Metal/semiconductor superlattices containing semimetallic ErSb nanoparticles in GaSb

Permalink
https://escholarship.org/uc/item/0zt089fh

Journal
Applied Physics Letters, 84(2)

ISSN
0003-6951

Authors
Hanson, M P
Driscoll, D C
Kadow, C
et al.

Publication Date
2004

Peer reviewed

eScholarship.org Powered by the California Digital Library
University of California

HTML ABSTRACT + LINKS

Metal/semiconductor superlattices containing semimetallic ErSb nanoparticles in GaSb

M. P. Hanson,[a] D. C. Driscoll, C. Kadow, and A. C. Gossard
Materials Department, University of California, Santa Barbara, California 93106-5050

(Received 1 August 2003; accepted 17 November 2003)

We demonstrate the growth by molecular beam epitaxy of a metal/semiconductor composite consisting of epitaxial semimetallic ErSb particles in a GaSb matrix. The ErSb nucleates in an island growth mode leading to the spontaneous formation of nanometer-sized particles. These particles are found to preferentially grow along a [011] direction on a (100) GaSb surface. The particles can be overgrown with GaSb to form an epitaxial superlattice consisting of ErSb particles between GaSb spacer layers. The size of the ErSb particles increases monotonically with the deposition. The carrier concentrations in the superlattices are found to be dependent on both the size and density of the ErSb particles. Smaller particles and closer layer spacings reduce the hole concentration in the film. © *2004 American Institute of Physics.* [DOI: 10.1063/1.1639932]

Epitaxial structures containing metallic particles buried within a semiconductor matrix have been demonstrated to be effective ways of manipulating the electrical properties of the host semiconductor. Superlattices consisting of ErAs particles and GaAs spacer layers have been shown to possess higher resistivity, higher electrical breakdown fields, and much shorter carrier lifetimes than pure GaAs.[1] These properties are ideal for devices that rely on high-speed photoconductors, such as high-speed photodetectors[2] and photomixers.[3] Recently, ErAs semimetallic particles have been placed at the interface of a GaAs $p-n$ junction and were shown to substantially enhance the tunneling current.[4] GaAs/ErAs superlattices have also been used as electrical isolation layers because of their high resistivity and ability to withstand a high electrical field.[5] A similar material that absorbs at longer wavelengths would be useful. Superlattices of ErAs and InGaAs lattice matched to InP have previously been used in an attempt to achieve such a material. Here we present an alternative approach using the GaSb/ErSb materials system, which may help circumvent problems of dark resistance and surface morphology encountered in the ErAs/InGaAs superlattices.[6–8]

The 0.73 eV direct band gap of the GaSb host material allows strong absorption at the wavelength of 1.55 μm. The semimetallic band structure of ErSb[9] and the small lattice mismatch of less than 0.2% with GaSb make ErSb a good choice for GaSb based metal/semiconductor composite structures. Like GaSb, ErSb has a cubic lattice, however, ErSb crystallizes in the rock-salt structure rather than the zinc blende structure of GaSb. Growth of epitaxial complete layers of ErSb on GaSb by molecular beam epitaxy (MBE) has previously been demonstrated.[10] In this letter we examine the growth regime prior to the formation of a complete film. In this regime the ErSb spontaneously forms nanometer-sized particles similar to ErAs on GaAs[11] and InGaAs.[6] We grow and study the properties of composite materials consisting of layers of self-assembled ErSb semimetallic particles within a GaSb matrix.

We grew GaSb/ErSb structures by solid-source MBE in a Varian Gen II machine. The ErSb growth rate was obtained from beam flux measurements based on previously published calibrations.[12] Depositions of ErSb are stated in monolayers (ML) as if the ErSb had grown in a layer-by-layer growth mode (1 ML of ErSb = 3 Å of film thickness). Superlattices consisting of small depositions of ErSb separated by GaSb spacer layers were investigated with x-ray diffraction, atomic force microscopy (AFM), and Hall effect. A diagram of the sample structure is shown in the inset of Fig. 1. Samples were grown on both (100)-oriented unintentionally p type GaSb substrates and (100)-oriented semi-insulating GaAs substrates with a half micron relaxed AlSb buffer layer. The AlSb buffer layer was grown at a substrate temperature of 570 °C. For the growth of the GaSb/ErSb superlattice the substrate temperature was reduced to 530 °C. The GaSb and AlSb layers were grown with Sb_2 from a valved cracker at a III/V ratio of 1:3. The ErSb was grown at a rate of 0.037

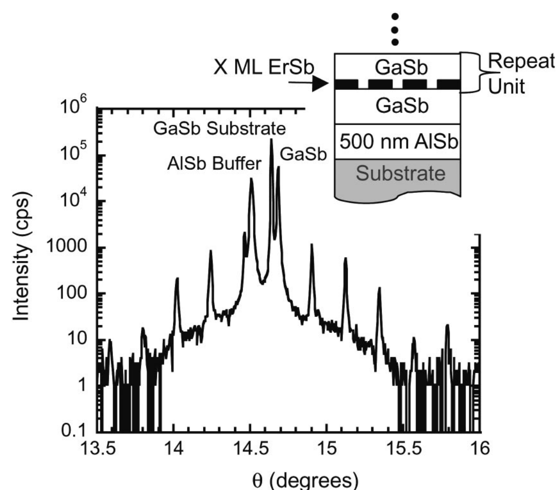

FIG. 1. θ–2θ x-ray diffraction pattern of a 30×20 nm GaSb 2 ML ErSb superlattice grown on a GaSb substrate. The inset shows the ErSb/GaSb superlattice structure.

[a]Electronic mail: micah@engineering.ucsb.edu

 © 2004 American Institute of Physics
Downloaded 27 Jan 2004 to 128.111.192.123. Redistribution subject to AIP license or copyright, see http://ojps.aip.org/aplo/aplcr.jsp

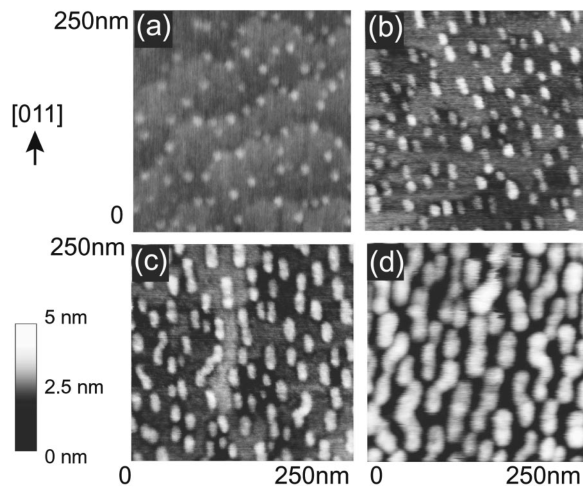

FIG. 2. AFM images of ErSb particles on a GaSb surface for (a) 0.1 ML of ErSb, (b) 0.5 ML of ErSb, (c) 1 ML of ErSb, and (d) 2.5 ML of ErSb. ErSb particles preferentially elongate along the [011] direction.

ML/s with Er:Sb ratio of 1:13. GaSb is then grown over the ErSb islands. This process is repeated to form a superlattice.

AFM images of the surface of the superlattices showed very little increase in roughness for ErSb depositions up to 2 ML over the reference GaSb sample. In addition, the reflective high-energy electron diffraction (RHEED) pattern of the GaSb surface after the growth of the superlattice maintained the same intensity and appearance as the surface prior to the superlattice. Both of these results indicate that the addition of ErSb particles has a minimal effect on the layer-by-layer growth of the GaSb. Figure 1 shows a (002) θ–2θ x-ray diffraction pattern of a 30 period superlattice with a 2 ML ErSb 20 nm GaSb repeat unit, (2 ML 30×20 nm) grown lattice matched to a GaSb substrate with a 500 nm AlSb buffer. Superlattice peaks are clearly visible, demonstrating good coherence in the growth direction.

In addition to the superlattice samples, four samples were grown for AFM study of ErSb particle formation. Uncovered depositions of 0.1, 0.5, 1, and 2.5 ML of ErSb on 500 nm of GaSb were grown on relaxed 500 nm AlSb buffers nucleated on semi-insulating GaAs substrates. AFM images of these samples are shown in Fig. 2. From the AFM images it is clear that the ErSb forms islands similar to those that have been observed for ErAs on both GaAs[11] and InGaAs.[6] It is also noted that the islands form preferentially along a [011] direction, which suggests that the Er adatoms migrate faster along this direction. This was also observed for ErAs grown on InGaAs[6] but not for ErAs on GaAs.[11,13] For the 0.1 ML deposition the height of the islands is between 5 and 9 Å and the average particle area was 70 nm^2 with a density of 1.1×10^{11} cm^{-2}. As the deposition is increased to 0.5 ML, the density of particles increases to about 2.2×10^{11} cm^{-2}, with the average particle area increasing to 120 nm^2. By increasing the deposition to 1 ML the particle density is reduced to about 1.5×10^{11} cm^{-2} while the average particle area increases to 300 nm^2. The height of the islands remained relatively constant between 10 and 16 Å (or about 4 ML) for these depositions. The particle density decreases as particles coalesce to form larger particles. This phenomenon continues in the 2.5 ML sample as the density is further reduced to 4×10^{10} cm^{-2} and the average particle area increases to 1300 nm^2.

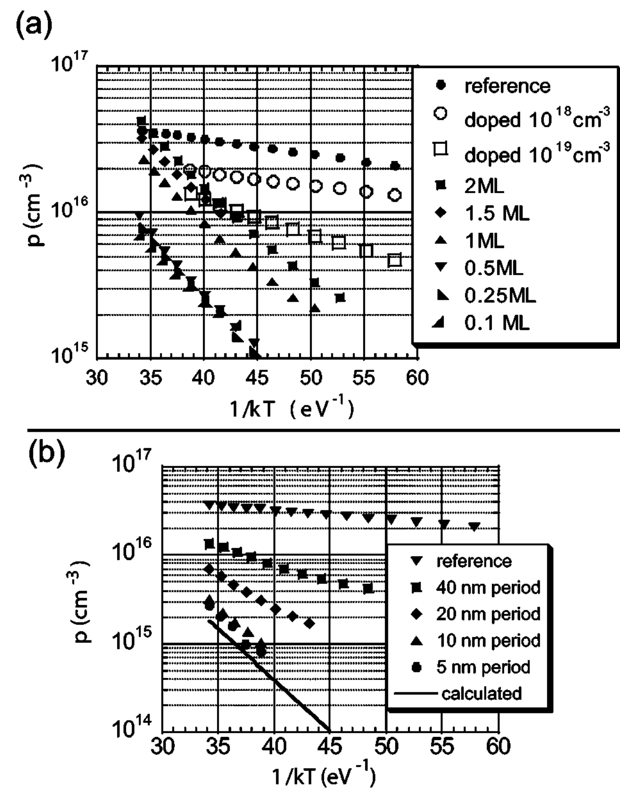

FIG. 3. The hole concentration in GaSb/ErSb superlattices vs $1/kT$ for (a) various ErSb depositions (in ML) in a 30×20 nm GaSb/ErSb superlattice as well as a GaSb reference sample and two bulk Er doped GaSb films and (b) various *period lengths* for GaSb/0.1 ML ErSb superlattices. The total thickness of the film was kept to 620 nm by adjusting the number of periods. The calculated line shows the calculated temperature dependence of the hole concentration if the Fermi level were uniformly pinned at the published Schottky barrier height of 500 meV below the conduction band (see Ref. 10).

Temperature dependent Hall measurements in the van der Pauw geometry were performed on the GaSb/ErSb superlattice samples grown on semi-insulating GaAs substrates to determine the in-plane bulk transport properties of the material. A GaSb reference sample was also grown under the same conditions with the same structure as the superlattice samples but containing no ErSb. The reference GaSb layer was measured to be p type with a hole concentration of 3.5×10^{16} cm^{-3} and mobility of 600 cm^2/V s at room temperature. This is consistent with the unintentionally p type behavior previously observed in GaSb which has been attributed to a defect in the GaSb crystal.[14] Figure 3(a) shows the hole concentration plotted versus $1/kT$, where k is Boltzmann's constant and T is the temperature, for various depositions of ErSb in 30×20 nm superlattices. In addition, the reference GaSb sample and two uniformly Er-doped GaSb samples with Er concentrations of 10^{18} and 10^{19} cm^{-3} are shown. Even though the 0.1 ML 30×20 nm superlattice has nearly the same average concentration of Er the two samples show a different temperature dependence of carrier concentration. The carrier concentrations vary exponentially with temperature and for the superlattice samples they are strongly dependent on particle size and density. The carrier concentration allows us to calculate the position of the Fermi level in the materials. A summary of calculated Fermi level,

Downloaded 27 Jan 2004 to 128.111.192.123. Redistribution subject to AIP license or copyright, see http://ojps.aip.org/aplo/aplcr.jsp

TABLE I. (a) Room temperature electrical properties for various ErSb depositions (Dep.) in a 30×20 nm superlattice and a reference GaSb sample. (b) Room temperature electrical properties for various *periods* in a 0.1 ML ErSb and GaSb superlattice. The number of periods was adjusted to maintain a constant film thickness of 620 nm.

(a)	Dep. (ML)	p (cm^{-3})	Mobility ($cm^2/V\,s$)	Resistivity (Ω cm)	Fermi level (meV)
	ref	3.3×10^{16}	577	0.34	124
	2	1.8×10^{16}	166	2.13	139
	1.5	1.5×10^{16}	171	2.53	145
	1	1.0×10^{16}	191	3.24	154
	0.5	3.4×10^{15}	205	9.23	183
	0.25	3.1×10^{15}	260	7.91	185
	0.1	3.1×10^{15}	297	7.05	185
(b)	Period (nm)	p (cm^{-3})	Mobility ($cm^2/V\,s$)	Resistivity (Ω cm)	Fermi level (meV)
	ref	3.3×10^{16}	577	0.34	124
	40	8.1×10^{15}	346	2.24	160
	20	3.1×10^{15}	297	7.05	185
	10	1.0×10^{15}	314	19.5	214
	5	8.2×10^{14}	235	32.6	220

carrier concentration, mobility, and resistivity is shown in Table I(a).

The ability to use small ErSb depositions to produce more insulating material allows for improved overgrowth of the GaSb layer, higher quality material, and higher carrier mobilities. The relatively high hole mobilities of 150–300 $cm^2/V\,s$ suggest that the transport mechanism is hole conduction through the semiconductor matrix rather than carriers hopping between the metallic particles. While the mechanism of the dependence of carrier concentration on particle size is not yet understood, a similar dependence on particle size has been observed in InGaAs/ErAs superlattices.[7,8] In both cases smaller particles have lower work functions and higher Fermi energies.

In Fig. 3(b), hole concentration versus $1/kT$ is plotted for various ErSb layer spacings. The thickness of each sample was kept constant by adjusting the number of periods so that the total thickness of the GaSb region was 620 nm, effectively increasing the density of particles. In addition to the measured data, a calculation of the hole concentration in GaSb is shown. This calculation assumes that the Fermi level was pinned at the published bulk Schottky barrier height between GaSb and ErSb of 500 meV below the conduction band[10] and assumes a density of states based on the GaSb effective mass coefficients of 0.25 for the heavy hole and 0.05 for the light hole. As the layers of ErSb particles are moved closer together, the hole concentration is reduced and it approaches the calculation. Table I(b) summarizes the carrier concentration, mobility, resistivity, and Fermi level for various ErSb layer spacings. The reduction of holes with decreasing layer spacing is consistent with an increase in the overlap of the depletion regions that surround the ErSb particles.

In summary, we have demonstrated the growth of a metal/semiconductor composite consisting of nanometer-sized ErSb particles in a GaSb matrix. The GaSb overgrowth planarizes after less than 40 Å of growth on top of a 0.1 ML deposition of ErSb as observed by RHEED. This allows ErSb layers to be placed as close as 5 nm apart without significant degradation of the material with an increasing numbers of periods. The particles were found to preferentially elongate along the [011] direction and to grow to about 4 ML in height before spreading out and merging to form larger particles. The carrier concentrations in the superlattices can be correlated to the microstructure of the material. This establishes a powerful way to control the properties of semiconductors by engineering of embedded nanostructures.

This work was supported by the Office of Naval Research. The authors would like to thank Herb Kroemer, Elliott Brown, and Gottfried Döhler for useful discussions.

[1] C. Kadow, A. W. Jackson, A. C. Gossard, J. E. Bowers, S. Matsuura, and G. A. Blake, Physica E (Amsterdam) **7**, 3510 (2000).
[2] Y. Chen, S. Williamson, T. Brock, F. W. Smith, and A. R. Calawa, Appl. Phys. Lett. **59**, 1984 (1991).
[3] E. R. Brown, F. W. Smith, and K. A. McIntosh, J. Appl. Phys. **73**, 1480 (1993).
[4] P. Pohl, F. Renner, M. Eckardt, A. Schwanhäusser, A. Friedrich, Ö. Yöksekdag, S. Malzer, G. H. Döhler, P. Kiesel, D. Driscoll, M. Hanson, and A. C. Gossard, Appl. Phys. Lett. **83**, 4035 (2003).
[5] A. Dorn, M. Peter, S. Kicin, T. Ihn, K. Ensslin, D. Driscoll, and A. C. Gossard, Appl. Phys. Lett. **82**, 2631 (2003).
[6] D. C. Driscoll, M. P. Hanson, E. Mueller, and A. C. Gossard, J. Cryst. Growth **251**, 243 (2003).
[7] M. P. Hanson, D. C. Driscoll, E. Mueller, and A. C. Gossard, Physica E (Amsterdam) **13**, 602 (2002).
[8] D. C. Driscoll, M. Hanson, C. Kadow, and A. C. Gossard, Appl. Phys. Lett. **78**, 1703 (2001).
[9] Q. G. Sheng, B. R. Cooper, and S. P. Lim, J. Appl. Phys. **73**, 5409 (1993).
[10] A. Guivarc'h, Y. Ballini, Y. Toudic, M. Minier, P. Auvray, B. Guenais, J. Ccaulet, B. Le Merdy, B. Lambert, and A. Regreny, J. Appl. Phys. **75**, 2876 (1994).
[11] C. Kadow, J. A. Johnson, K. Kolstad, J. P. Ibbetson, and A. C. Gossard, J. Vac. Sci. Technol. B **18**, 2197 (2000).
[12] C. Kadow, S. B. Fleischer, J. P. Ibbetson, J. E. Bowers, A. C. Gossard, J. W. Dong, and C. J. Palmstrom, Appl. Phys. Lett. **75**, 3548 (1999).
[13] C. Kadow, J. A. Johnson, K. Kolstad, and A. C. Gossard, J. Vac. Sci. Technol. B **21**, 29 (2003).
[14] P. S. Dutta, H. L. Bhat, and V. Kumar, J. Appl. Phys. **81**, 5821 (1997).

Downloaded 27 Jan 2004 to 128.111.192.123. Redistribution subject to AIP license or copyright, see http://ojps.aip.org/aplo/aplcr.jsp